Available online at www.sciencedirect.com
ScienceDirect
Trans. Nonferrous Met. Soc. China 31(2021) 555−564
Transactions of Nonferrous Metals Society of China
www.tnmsc.cn

Hydrometallurgical process for recovery of Zn, Pb, Ga and Ge from Zn refinery residues

Shuai RAO[1,2,3], Zhi-qiang LIU[1,2,3], Dong-xing WANG[1,2,3], Hong-yang CAO[1,2,3], Wei ZHU[1,2,3], Kui-fang ZHANG[1,2,3], Jin-zhang TAO[1,2,3]

1. Research Institute of Rare Metals, Guangdong Academy of Sciences, Guangzhou 510650, China;
2. State Key Laboratory of Separation and Comprehensive Utilization of Rare Metals, Guangdong Academy of Sciences, Guangzhou 510650, China;
3. Guangdong Province Key Laboratory of Rare Earth Development and Application, Guangdong Academy of Sciences, Guangzhou 510650, China

Received 3 March 2020; accepted 28 October 2020

Abstract: Zn, Pb, Ga and Ge were separated and recovered from zinc refinery residues by stepwise leaching. In the first stage, by leaching with H_2SO_4 media, more than 90% of Zn and 99% of Ga were dissolved, leaving 92% of Ge in the leaching residue. In the second stage, by leaching with HCl media, approximately 99% of Pb and less than 2% of Ge were selectively dissolved. Finally, the remaining 90% of Ge was extracted in 1 mol/L NaOH solution by destroying the correlation between SiO_2 and Ge. XRD pattern of the leaching residue demonstrated that $ZnSO_4·H_2O$, $PbSO_4$ and SiO_2 were removed sequentially through the stepwise leaching. The proposed process achieved high recoveries of Zn, Pb, Ga and Ge, thus presenting a potential industrial application.

Key words: zinc refinery residues; gallium; germanium; stepwise leaching

1 Introduction

Germanium (Ge) and gallium (Ga) are considered as strategic metals in many countries owing to their wide applications in high-tech fields such as semiconductors, optical fibers and solar cells [1−4]. However, geological and mineralogical studies have shown that it is difficult to find independent deposits enriched with Ga and Ge [5,6]. Currently, Ga and Ge are mainly extracted from non-ferrous metal residues [7−10] or secondary resources [11,12]. The ZnS ores located in Guangdong province contain relatively high contents of Ga and Ge [13,14]. Based on the properties of the raw material, pressure leaching is applied to treating the minerals for recovering Zn, Ga and Ge. During pressure leaching, almost all Zn, Ga and Ge are dissolved in the leaching solution. Zinc powder is then used as the reducing agent to remove Pb and Fe during the subsequent purification procedure. Ga and Ge (0.1−0.5 wt.%) are also enriched in Zn refinery residues, which usually contain large amounts of Pb and Fe [15,16].

Currently, Ga and Ge are extracted from zinc plant residues by hydrometallurgical methods owing to high economic benefits and low environment pollution [17−19]. However, since Ga and Ge are closely correlated with Fe and Si, the recoveries of Ga and Ge are relatively low. During sulfuric acid leaching, the formation of silica gel results in a deteriorating filtration performance and significant loss of Ga and Ge [20]. To avoid the

Corresponding author: Zhi-qiang LIU; Tel: +86-20-61086372; E-mail: 1031494987@qq.com
DOI: 10.1016/S1003-6326(21)65517-6

problem, hydrofluoric acid has been supplemented to sulfuric acid solutions to enhance the leaching rates of Ga and Ge [21]. However, the subsequent defluorination procedure constrains its commercial applications. Alkaline leaching has also been proposed to recover Ga and Ge [22]. Although a relatively high recovery of Ga and Ge is obtained, a large amount of sodium hydroxide is consumed owing to the dissolution of Pb and Si [23]. Organic weak acids provide milder leaching conditions than mineral acids; therefore, they exhibit a high selectivity [24]. LIU et al [25] researched the recovery of Ga and Ge from Zn refinery residues using an oxalic acid solution after selectively removing Cu and Zn in a sulfuric acid solution. Although this method can achieve high leaching rates of Ga and Ge, it is difficult to regenerate the leaching agent, resulting in a high production cost. In general, considering environmental conservation and process efficiency, there is no appropriate technology for the comprehensive recovery of valuable metals, including Zn, Pb, Ga and Ge, from Zn refinery residues.

In this study, based on the properties of Zn refinery residues, stepwise leaching is proposed for the comprehensive recovery of Zn, Pb, Ga and Ge from Zn refinery residues. Firstly, Zn and Ga are dissolved in a sulfuric acid solution through controlled suitable leaching conditions, leaving behind Ge and Pb in the leaching residue. The resulting leaching solution can be further processed by adjusting the pH of the leaching solution to a weak acid environment for an effective separation of Zn and Ga. Secondly, Pb is selectively removed in a hydrochloric acid solution based on the complexation between Pb^{2+} and Cl^{-}. Moreover, a $PbCl_2$ product can be obtained through cooling crystallization. Finally, Ge is effectively extracted in a sodium hydroxide solution by destroying the embedded correlation between Ge and silica. The stepwise leaching method is a novel technology for the effective recovery of valuable metals from Zn refinery residues, with the potential to be applied on an industrial scale.

2 Experimental

2.1 Materials

The Zn refinery residue was obtained from a Zn metallurgy enterprise located in Shaoguan city, Guangdong province, China. Before conducting leaching, the material was dried, grounded and sieved to a particle size below 100 μm. The main elemental content of the residue was determined by inductively coupled plasma-atomic emission spectrometry (ICP-AES). Table 1 shows that the residue mainly contains Zn, Pb, Fe and Si. The contents of Ga and Ge are 0.15 wt.% and 0.47 wt.%, respectively.

Table 1 Main elemental contents of Zn refinery residue (wt.%)

Zn	Pb	Fe	Si	Ga	Ge
5.93	4.18	6.30	12.6	0.15	0.47

The main phases of the Zn refinery residue were determined by X-ray diffraction (XRD). As shown in Fig. 1, the main diffraction peaks were related to some obvious phases, including SiO_2, $ZnSO_4·H_2O$, $PbSO_4$ and $ZnFe_2O_4$. No other characteristic peaks corresponding to Ga or Ge phases were detected, owing to their low contents.

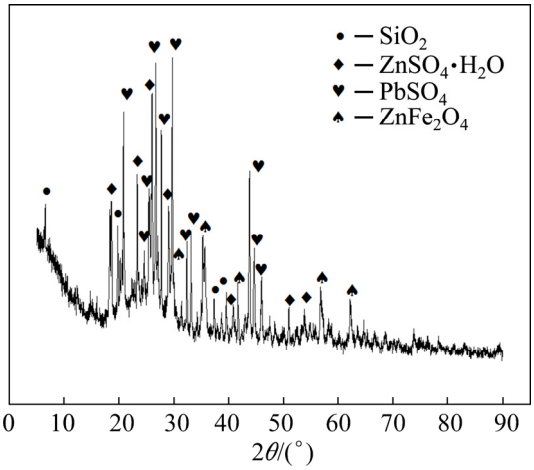

Fig. 1 XRD pattern of Zn refinery residue

Figure 2 shows the SEM image and elemental surface scanning images of the Zn refinery residue. The residue was mainly composed of many tiny dark particles representing SiO_2. Some large blocky-shaped particles suggesting various phases were also observed. The brightest particle can be viewed as $PbSO_4$, owing to the enrichment of Pb. Similarly, Fe and Zn were concentrated in some gray particles, confirming the presence of $ZnFe_2O_4$. The distributions for Ga and Ge were very sparse due to their low contents.

2.2 Experimental procedure

Based on the properties of Zn refinery residue, an environmentally friendly and economical process was proposed for the efficient recovery of Zn, Pb, Ga and Ge. The integrated process flow comprises three procedures, as shown in Fig. 3, namely, Zn and Ga leaching in a H_2SO_4 solution, Pb recovery in a HCl solution, and Ge extraction in a NaOH solution. After Zn and Ga leaching, the pH of the leaching solution was adjusted to weak acid for the separation of Zn and Ga by adding ZnO. During Pb recovery, soluble $PbCl_4^{2-}$ complex was transformed into $PbCl_2$ precipitate through dilution and cooling crystallization. The crystalline mother solution was regenerated by adding $CaCl_2$. The pH of the leaching solution obtained from Ge extraction was adjusted to a weak alkaline condition for the separation of Ge and Si by adding HCl. All leaching experiments were performed in a beaker immersed in a water bath with a thermostat, equipped with a magnetic stirrer. All chemical reagents used were analytical grade.

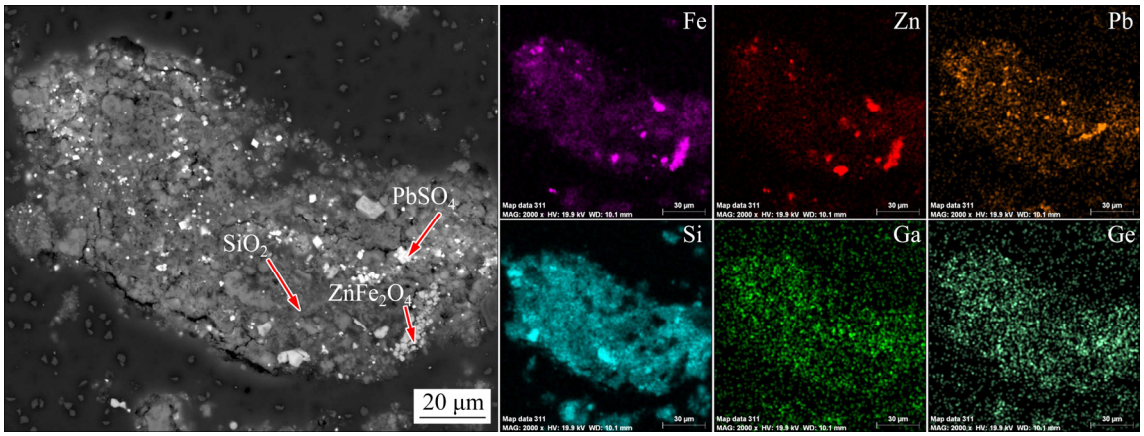

Fig. 2 SEM image and main elemental surface scanning images of Zn refinery residue

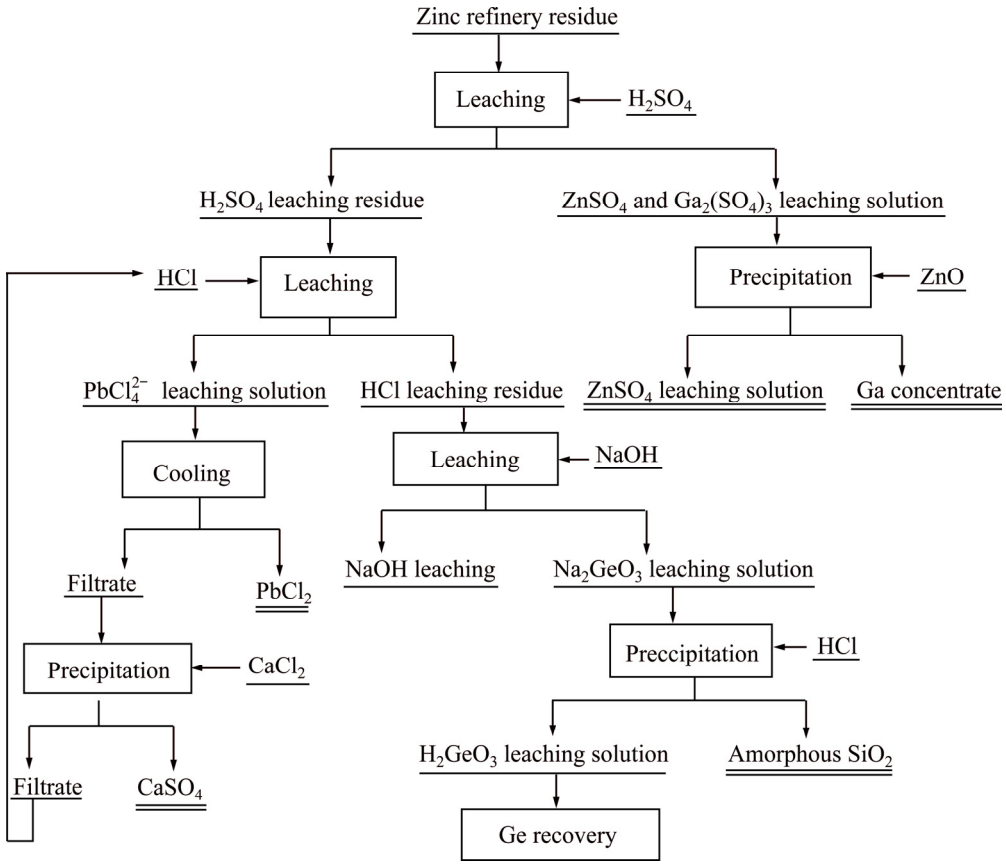

Fig. 3 Principal flow sheet for recovering valuable metals from Zn refinery residue

2.3 Analytical methods

The phases of the material and leaching residue were determined using a Rigaku TTRAX-3 X-ray diffraction instrument (40 kV, 30 mA, 10 (°)/min). The contents of the main elements, including Zn, Pb, Fe, Ga, Ge and Si, were determined using an inductively coupled plasma-atomic emission spectrometer (Thermo Electron IRIS Intrepid II XSP). The morphology and chemical composition of the samples were analyzed through SEM−EDS (SEM, JEOL, Ltd., JSM−6360LV).

3 Results and discussion

3.1 Zn and Ga leaching in H_2SO_4 solution

Owing to the formation of Ge−silica gel and $PbSO_4$ precipitate in a H_2SO_4 solution, sulfuric acid leaching mainly focuses on the leaching efficiency of Zn and Ga. Moreover, the separation of Zn and Ga should also be considered after the leaching is completed. The φ–pH diagram for a Zn−Ga−Fe−H_2O system has been depicted using the HSC 6.0. As illustrated in Fig. 4, Zn^{2+}, Ga^{3+} and Fe^{3+} were predominant under the acidic conditions, suggesting that sulfuric acid was an effective leaching agent to extract Zn and Ga. However, Zn, Ga and Fe each presented a different pH of hydrolysis precipitation. The precipitation of Ga^{3+} and Fe^{3+} in the form of $Fe(OH)_3$ and $Ga(OH)_3$ could occur at a pH above 3.0, while soluble Zn^{2+} existed in the solution at a pH below 6.0. Therefore, an effective separation of Zn and Ga could be obtained by adjusting the pH of the leaching solution to be 3.0−6.0.

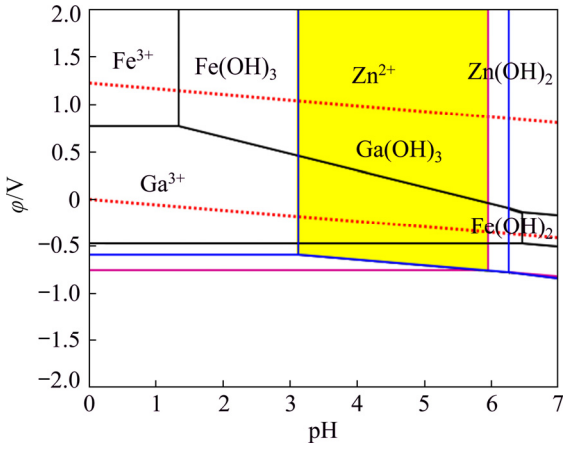

Fig. 4 φ–pH diagram for Zn−Ga−Fe−H_2O system at 25 °C ($\alpha(Zn^{2+})$=1, $\alpha(Fe^{3+})$=1, $\alpha(Ga^{3+})$=0.01)

Based on the above analyses, the effect of sulfuric acid concentration on the leaching process was investigated in detail. The other leaching conditions included a liquid solid ratio of 10 mL/g, reaction temperature of 80 °C, and leaching time of 2 h. As shown in Fig. 5, increasing the sulfuric acid concentration to 2 mol/L improved the leaching rate of Ga significantly. The Ga leaching rate approached 100% in a 2 mol/L H_2SO_4 solution. Moreover, large amounts of Zn and Fe dissolved in the leaching solution, whereas the Ge leaching rate was relatively low due to the formation of Ge−silica gel. Therefore, a suitable sulfuric acid concentration of 2 mol/L should be selected for optimal leaching of Zn and Ga.

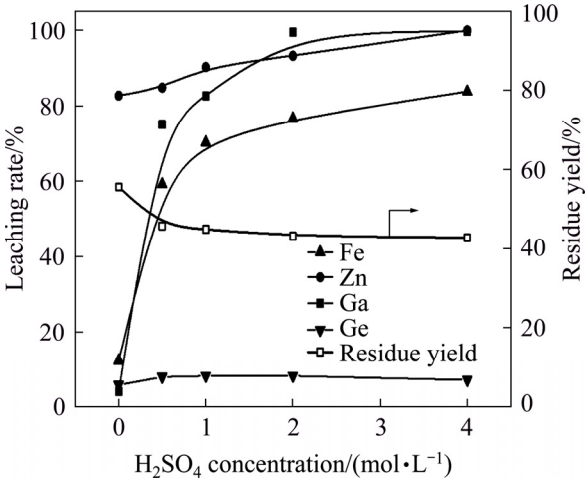

Fig. 5 Effect of H_2SO_4 concentration on leaching rates of Zn, Fe, Ga and Ge

Table 2 lists the main elemental content of the leaching residue obtained in a 2 mol/L H_2SO_4 solution. It can be seen that Zn, Fe and Ga decreased significantly, whereas Pb, Si and Ge increased in the H_2SO_4 leaching residue. The XRD pattern of the H_2SO_4 leaching residue is shown in Fig. 6. Compared with the results in Fig. 1, the characteristic peaks of $ZnSO_4 \cdot H_2O$ disappeared and the remaining phases contained $ZnFe_2O_4$, SiO_2 and $PbSO_4$. Figure 7 presents the SEM image of the H_2SO_4 leaching residue. Based on the results of the EDS analyses from Table 3, the blocky-shaped particles given by Spots 1 and 2 were confirmed as $PbSO_4$ and $ZnFe_2O_4$, respectively. These tiny dark particles (Spots 3, 4, and 5) were viewed as an enriching Si phase. More importantly, these enriching Si particles exhibited a high Ge content.

Table 2 Main elemental contents of leaching residue obtained in 2 mol/L H_2SO_4 solution (wt.%)

Zn	Pb	Fe	Si	Ga	Ge
1.49	9.64	1.52	26.1	0.01	1.03

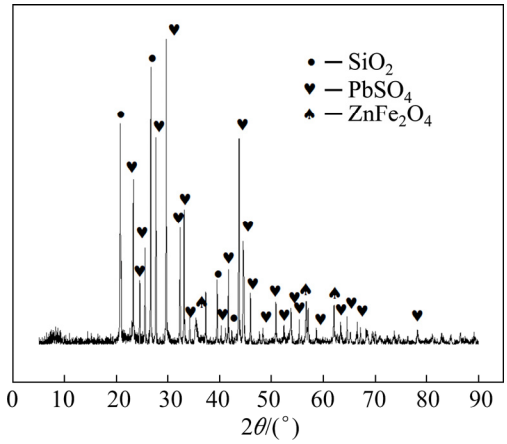

Fig. 6 XRD pattern of H_2SO_4 leaching residue

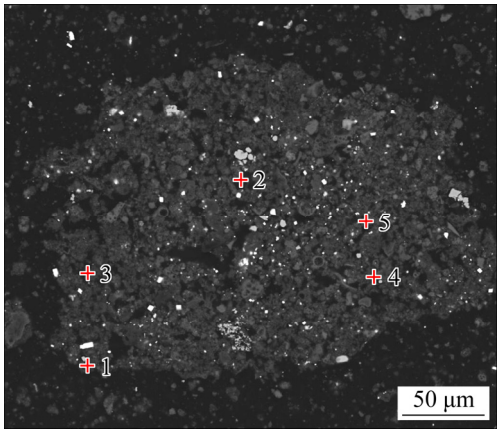

Fig. 7 SEM image of H_2SO_4 leaching residue

Table 3 Chemical composition of selected particles shown in Fig. 7 (wt.%)

Element	Spot 1	Spot 2	Spot 3	Spot 4	Spot 5
O	20.17	27.54	50.98	45.47	45.01
S	9.87	–	3.51	–	4.06
Zn	–	27.01	0.6	0.84	2.29
Pb	69.69	–	–	10.87	10.09
Fe	–	41.44	1.82	0.9	2.11
Si	–	0.84	37.15	36.51	30.08
Ga	–	–	–	–	–
Ge	–	0.01	2.02	2.18	2

Once the leaching was completed, Ga and Fe were deposited as $Ga(OH)_3$ and $Fe(OH)_3$ by adjusting the pH of the leaching solution to 4.0. The resulting $ZnSO_4$ solution could be returned to the Zn recovery procedure, while the precipitate was further treated to extract Ga. The precipitate obtained in this study exhibited an amorphous phase structure, as shown in Fig. 8. The contents of Fe and Ga in the precipitate were 30.08 and 1.00 wt.%, respectively, suggesting that Ga in the precipitate was over five times higher than that in the material.

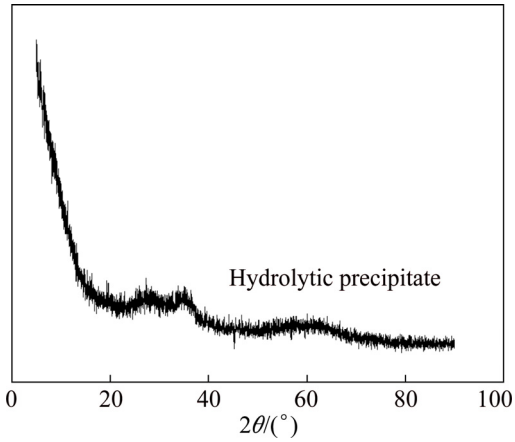

Fig. 8 XRD pattern of precipitate obtained from H_2SO_4 leaching solution

3.2 Pb recovery in HCl solution

After selective dissolution of Zn, Ga and Fe, the leaching residue was mainly composed of Pb, Ge and Si. Due to the formation of soluble $Pb(OH)_4^{2-}$ complex in an alkaline solution, it was necessary to remove Pb before extracting Ge. Based on the complexation between Pb^{2+} and Cl^-, HCl was selected as a suitable leaching agent. The distribution curves of the Pb species with different Cl^- concentrations were constructed using the Medusa software. As shown in Fig. 9, $PbCl_2$ precipitate predominated under a relatively low Cl^- concentration condition, while an increased Cl^- concentration was beneficial for the formation of soluble $PbCl_4^{2-}$ complex. This suggests that Pb recovery should be conducted under larger leaching agent concentration and higher liquid-to-solid ratio conditions. Therefore, the leaching process was performed with a liquid-to-solid ratio of 20 mL/g at 90 °C for 2 h. Figure 10 shows the effect of HCl concentration on the leaching rates of Pb and Ge. The leaching rate of Pb enhanced with an increasing HCl concentration from 0.5 to 2 mol/L. Almost all of the $PbSO_4$ dissolved in a 2 mol/L HCl solution, with the Ge leaching rate below 2%.

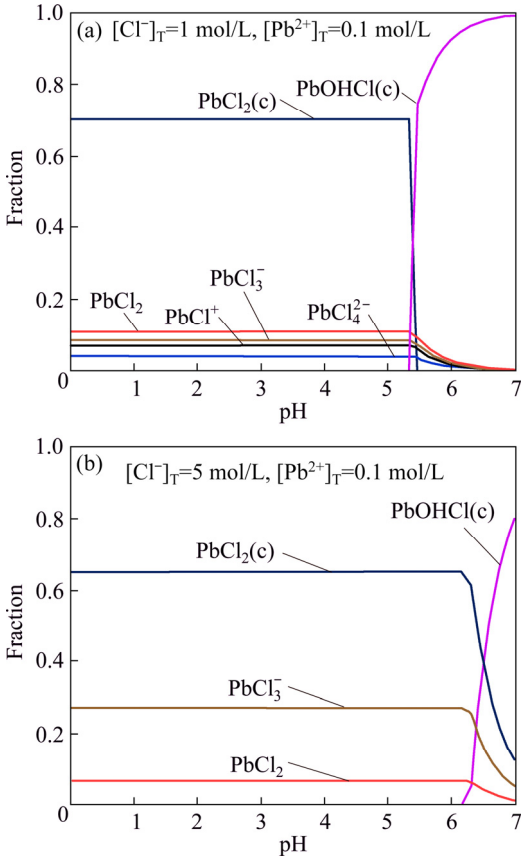

Fig. 9 Distribution of Pb species at different pH for Pb^{2+}–Cl^-–H_2O system at 25 °C

Table 4 lists the main elemental contents of the leaching residue. It can be seen that Ge increased to above 1.37 wt.% in the leaching residue, whereas the content of Pb reduced to below 0.1 wt.%. The main phases of the leaching residue were SiO_2 and $ZnFe_2O_4$, as shown in Fig. 11. Compared with Fig. 7, Fig. 12 shows that the brightest particles representing the $PbSO_4$ phase were seldom observed. Moreover, there was a close correlation between Ge and Si based on the Ge–Si surface distribution diagram.

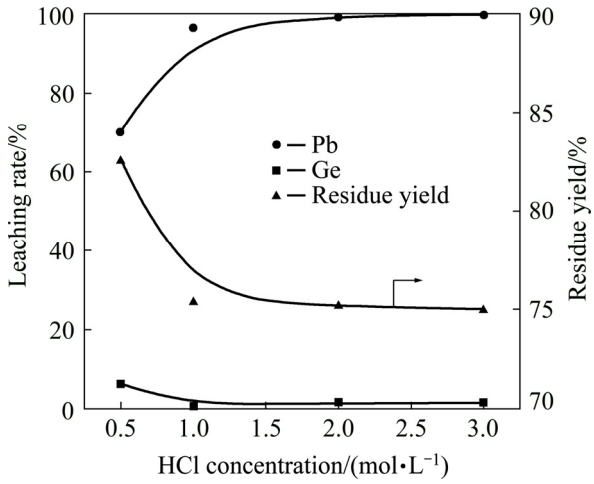

Fig. 10 Effect of HCl concentration on leaching rates of Pb and Ge

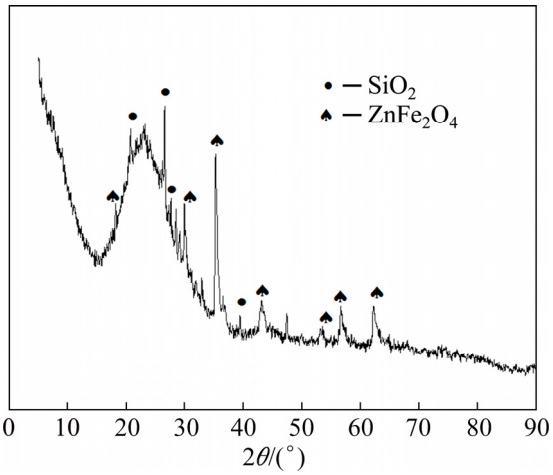

Fig. 11 XRD pattern of HCl leaching residue

Table 4 Main elemental contents of leaching residue obtained in 2 mol/L HCl solution (wt.%)

Zn	Pb	Fe	Si	Ga	Ge
1.29	0.078	1.31	30	0.007	1.37

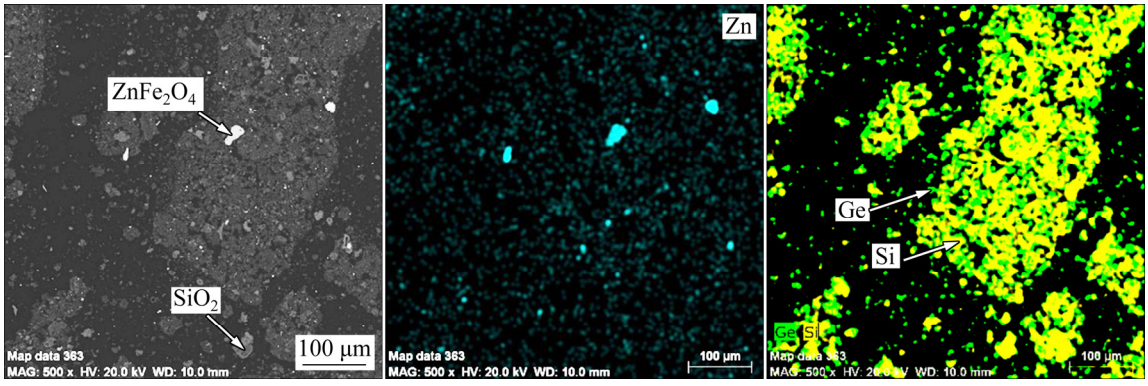

Fig. 12 SEM image and Ge–Si surface distribution of leaching residue obtained in 2 mol/L HCl solution

After completion of the Pb leaching, it is necessary to recover Pb from the leaching solution. A $PbCl_4^{2-}$ complex can be transformed into $PbCl_2$ precipitate by decreasing the reaction temperature and Cl^- concentration [26]. Therefore, the leaching solution was processed by dilution and cooling. Then, the $PbCl_2$ product was obtained by liquid−solid separation. The Pb content in the solution lowered from 4.78 to 1.79 g/L, suggesting that approximately 37.4% of Pb remained in the leaching solution. More than 60% of Pb was recovered in the form of $PbCl_2$, as shown in Fig. 13. The $PbCl_2$ product containing 74.3 wt.% Pb exhibited a high purity without any additional characteristic peaks. As shown in Fig. 14, after cooling crystallization, the resulting solution was regenerated by adding $CaCl_2$ to remove SO_4^{2-} by precipitation reaction between SO_4^{2-} and Ca^{2+}, allowing for the regenerated solution to be used in the subsequent lead removing procedure.

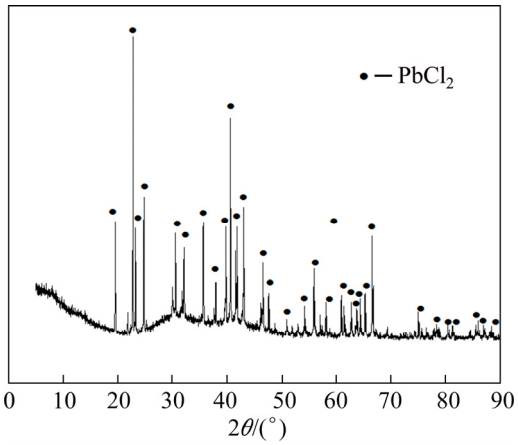

Fig. 13 XRD pattern of $PbCl_2$ product from HCl leaching solution

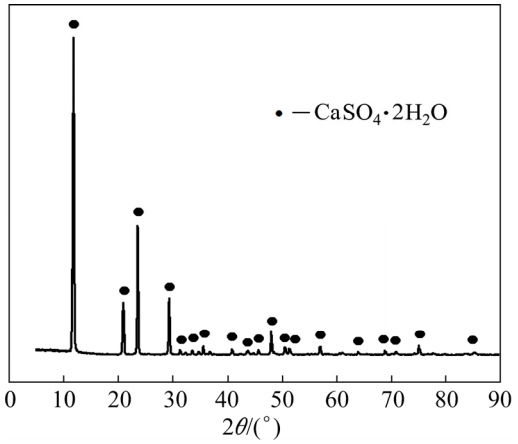

Fig. 14 XRD pattern of precipitate obtained from regeneration of leaching agent

3.3 Extraction of Ge in NaOH solution

To remove silica−germanium gel, NaOH is used as the leaching agent to effectively extract Ge. Leaching experiments were conducted at 80 °C with a liquid solid ratio of 20 mL/g for 2 h. Figure 15 shows the effect of NaOH concentration on the leaching rates of Ge and Si. An increased NaOH concentration significantly improved the dissolution efficiency of Ge and Si. More than 99% of Ge and 90% of Si were dissolved in 1 mol/L NaOH solution. Table 5 lists the main elemental contents of the NaOH leaching residue. Fe and Zn increased in the leaching residue, whereas Ge decreased to 0.06%. The XRD pattern, shown in Fig. 16, indicates the main phases of the leaching residue to be SiO_2, ZnS and $ZnFe_2O_4$. Compared

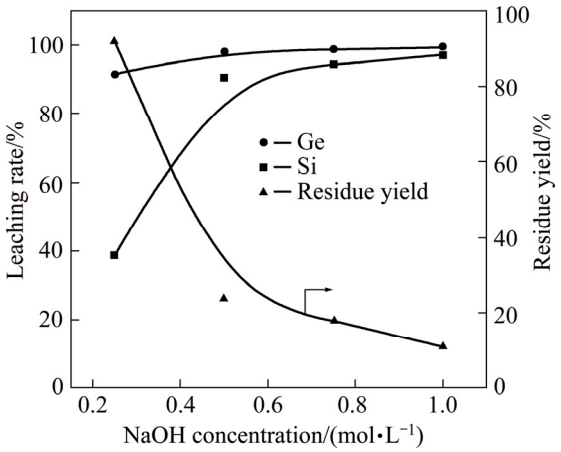

Fig. 15 Effect of NaOH concentration on leaching rates of Si and Ge

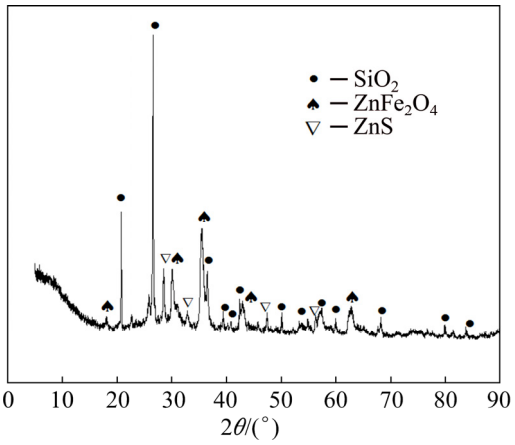

Fig. 16 XRD pattern of NaOH leaching residue

Table 5 Main elemental contents of leaching residue obtained in 1 mol/L NaOH solution (wt.%)

Zn	Fe	Pb	Si	Ga	Ge
6.81	7.1	0.11	7.69	0.01	0.06

with Fig. 8, new characteristic peaks of ZnS were observed owing to an increased Zn content in the leaching residue. Figure 17 shows the SEM image and main elemental surface distribution of the alkaline leaching residue. The tiny silica−germanium gel particles dissolved entirely, and the remaining particles, including ZnS, $ZnFe_2O_4$ and SiO_2, were large, preventing adequate dissolution through atmospheric leaching.

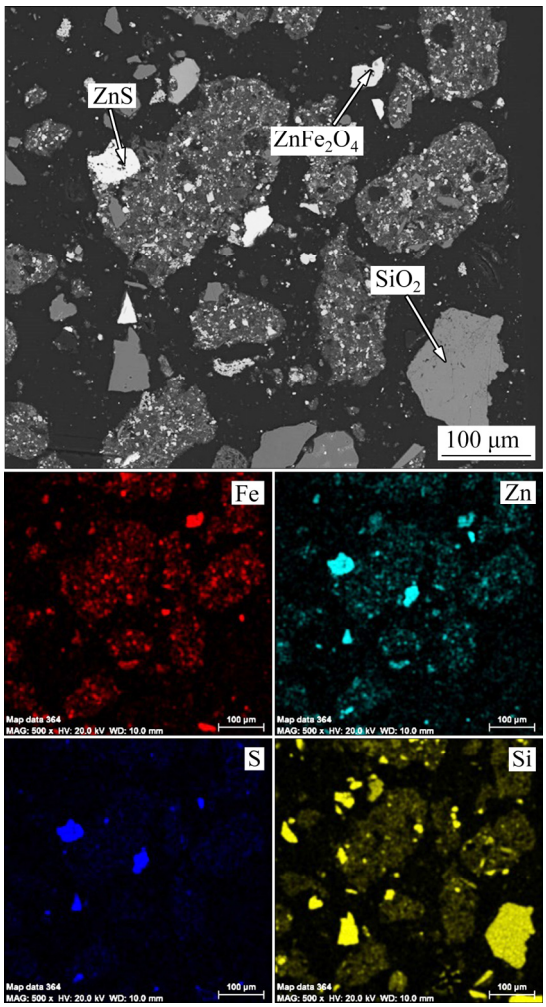

Fig. 17 SEM image and main elemental surface scanning maps of leaching residue

After Ge leaching, it is necessary to separate Ge and Si from the leaching solution owing to the dissolution of SiO_2. According to the φ−pH diagram for the Ge−Si−H_2O system in Fig. 18, Ge−silica gel can be destroyed by promoting the formation of soluble $HGeO_3^-$ and $SiO(OH)_3^-$ in an alkaline solution. After the leaching is complete, the precipitation of Si in the form of amorphous silicon dioxide can occur by adjusting the pH to be 6.0−12.0, allowing for an effective separation of Ge and Si. Therefore, in this study, the pH of the alkaline leaching solution was adjusted to be 9.0 by adding 2 mol/L HCl. The Si content in the leaching solution lowered to less than 0.3 g/L, as shown in Table 6, allowing for an excellent Ge−Si separation efficiency. Moreover, Zn, Pb and Fe were also adequately removed. The leaching solution could then be used to recover Ge through precipitation or solvent extraction. The white precipitate obtained from the Ge−Si separation procedure was amorphous silicon dioxide and, therefore, no obvious characteristic peaks were observed, as shown in Fig. 19.

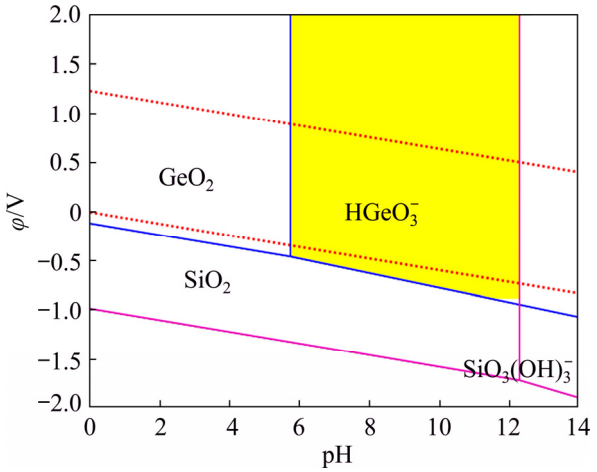

Fig. 18 φ−pH diagram for Ge−Si−H_2O system at 25 °C ($\alpha(Si^{4+})$=1, $\alpha(Ge^{4+})$=0.01)

Table 6 Main elemental contents of leaching solution adjusted to pH 9.0 (mg/L)

Zn	Pb	Fe	Si	Ga	Ge
<0.5	<0.5	<0.5	268.1	<0.5	254.1

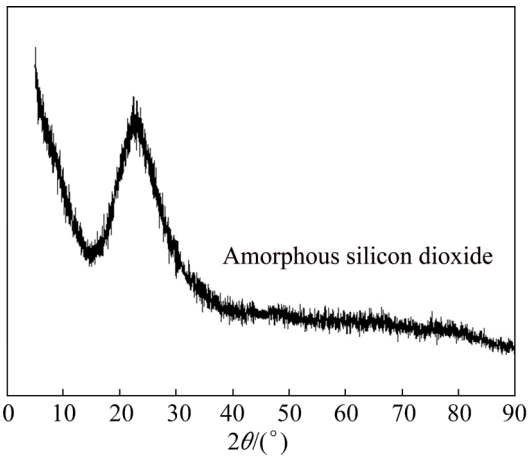

Fig. 19 XRD pattern of white precipitate obtained during Ge and Si separation

4 Conclusions

(1) More than 90% of Zn and 99% of Ga were leached in a 2 mol/L H_2SO_4 solution with a liquid–solid ratio of 10 mL/g at 80 °C after 2 h, leaving approximately 92% of Ge in the leaching residue. The content of Ga in the precipitate was over 5 times higher than in the raw material.

(2) About 99% of Pb and less than 2% of Ge were dissolved in a 2 mol/L HCl solution with a liquid-to-solid ratio of 20 mL/g at 90 °C for 2 h. A $PbCl_2$ byproduct with a high purity was obtained by cooling crystallization.

(3) During alkaline leaching, the remaining 90% of the Ge was extracted in a 1 mol/L NaOH solution with a liquid-to-solid ratio of 20 mL/g at 80 °C for 2 h. An effective Ge−Si separation was conducted by adjusting the pH of the leaching solution to 9.0.

Acknowledgments

The authors are grateful for the financial supports from the National Natural Science Foundation of China (51804083, 51704081), the National Key Research and Development Project (2018YFC1903104), the Natural Science Foundation of Guangdong Province, China (2019A1515011628), the Science and Technology Planning Project of Guangzhou (201904010106) of China, and Guangdong Academy of Science Doctor Special Program of China (2020GDASYL-0104027, 2019GDASYL-0105079, 2019GDASYL-0302011, 2019GDASYL-0402003).

References

[1] FTHENAKIS V, WANG Wen-ming, KIM H C. Life cycle inventory analysis of the production of metals used in photovoltaics [J]. Renewable and Sustainable Energy Reviews, 2009, 13(3): 493−517.

[2] CAROLAN D. Recent advances in germanium nanocrystals: Synthesis, optical properties and applications [J]. Progress in Materials Science, 2017, 90: 128−158.

[3] FRENZEL M, MIKOLAJCZAK C, REUTER M A, GUTZMER J. Quantifying the relative availability of high-tech by-product metals−The cases of gallium, germanium and indium [J]. Resources Policy, 2017, 52: 327−335.

[4] SIONTAS S, LI D, WANG H, A. V. P. S A, ZASLAVSKY A, PACIFICI D. High-performance germanium quantum dot photodetectors in the visible and near infrared [J]. Materials Science in Semiconductor Processing, 2019, 92: 19−27.

[5] LU Fang-hai, XIAO Tang-fu, LIN Jian, NING Zeng-ping, LONG Qiong, XIAO Li-hua, HUANG Fang, WANG Wan-kun, XIAO Qing-xiang, LAN Xiao-long, CHEN Hai-yan. Resources and extraction of gallium: A review [J]. Hydrometallurgy, 2017, 174: 105−115.

[6] MOSKALYK R R. Review of germanium processing worldwide [J]. Minerals Engineering, 2004, 17(3): 393−402.

[7] FRENZEL M, HIRSCH T, GUTZMER J. Gallium, germanium, indium, and other trace and minor elements in sphalerite as a function of deposit type: A meta-analysis [J]. Ore Geology Reviews, 2016, 76: 52−78.

[8] LU Fang-hai, XIAO Tang-fu, LIN Jian, LI An-jing, LONG Qiong, HUANG Fang, XIAO Li-hua, LI Xiang, WANG Jia-wei, XIAO Qing-xiang, CHEN Hai-yan. Recovery of gallium from Bayer red mud through acidic leaching-ion exchange process under normal atmospheric pressure [J]. Hydrometallurgy, 2018, 175: 124−132.

[9] KUL M, TOPKAYA Y. Recovery of germanium and other valuable metals from zinc plant residues [J]. Hydrometallurgy, 2008, 92(3): 87−94.

[10] MACÍAS-MACÍAS K Y, CENICEROS-GÓMEZ A E, GUTIÉRREZ-RUIZ M E, GONZÁLEZ-CHÁVEZ J L, MARTÍNEZ-JARDINES L G. Extraction and recovery of the strategic element gallium from an iron mine tailing [J]. Journal of Environmental Chemical Engineering, 2019, 7(2): 102964.

[11] ZHOU Jia-zhi, ZHU Neng-wu, LIU Huang-rui, WU Ping-xiao, ZHANG Xiao-ping, ZHONG Zu-qi. Recovery of gallium from waste light emitting diodes by oxalic acidic leaching [J]. Resources, Conservation and Recycling, 2019, 146: 366−372.

[12] CHEN Wei-Sheng, CHANG Bi-Cheng, CHIU Kai-Lun. Recovery of germanium from waste optical fibers by hydrometallurgical method [J]. Journal of Environmental Chemical Engineering, 2017, 5(5): 5215−5221.

[13] LIU Fu-peng, LIU Zhi-hong, LI Yu-hu, LIU Zhi-yong, LI Qi-hou, WEN Da-min. Sulfuric leaching process of zinc powder replacement residue containing gallium and germanium [J]. The Chinese Journal of Nonferrous Metals, 2016, 26(4): 908−918. (in Chinese)

[14] LIU Fu-peng, LIU Zhi-hong, LI Yu-hu, LIU Zhi-yong, LI Qi-hou. Leaching mechanism of zinc powder replacement residue containing gallium and germanium by high pressure acid leaching [J]. The Chinese Journal of Nonferrous Metals, 2014, 24(4): 1091−1098. (in Chinese)

[15] LIU Fu-peng, LIU Zhi-hong, LI Yu-hu, LIU Zhi-yong, LI Qi-hou, ZENG Li. Extraction of gallium and germanium from zinc refinery residues by pressure acid leaching [J]. Hydrometallurgy, 2016, 164: 313−320.

[16] LIU Fu-peng, LIU Zhi-hong, LI Yu-hu, WILSON B P, LUNDSTRÖM M. Recovery and separation of gallium (III) and germanium (IV) from zinc refinery residues: Part I: Leaching and iron (III) removal [J]. Hydrometallurgy, 2017, 169: 564−570.

[17] WU Xue-lan, WU Shun-ke, QIN Wen-qing, MA Xi-hong, NIU Yin-jian, LAI Shao-shi, YANG Cong-ren, JIAO Fen, REN Liu-yi. Reductive leaching of gallium from zinc residue [J]. Hydrometallurgy, 2012, 113−114: 195−199.

[18] LIANG Duo-qiang, WANG Ji-kun, WANG Yun-hua.

Difference in dissolution between germanium and zinc during the oxidative pressure leaching of sphalerite [J]. Hydrometallurgy, 2009, 95(1): 5−7.
[19] ZHANG Li-bo, GUO Wen-qian, PENG Jin-hui, LI Jing, LIN Guo, YU Xia. Comparison of ultrasonic-assisted and regular leaching of germanium from by-product of zinc metallurgy [J]. Ultrasonics Sonochemistry, 2016, 31: 143−149.
[20] HARBUCK D D. Optimization of gallium and germanium extraction from hydrometallurgical zinc residue [J]. Light Metals, 1989: 984−989.
[21] HARBUCK D D. Increasing germanium extraction from hydrometallurgical zinc residues [J]. Mining, Metallurgy & Exploration, 1993, 10(1): 1−4.
[22] TORMA A E. Method of extracting gallium and germanium [J]. Mineral Processing and Extractive Metallurgy Review, 1991, 3: 235−258.
[23] RAO Shuai, WANG Dong-xing, LIU Zhi-qiang, ZHANG Kui-fang, CAO Hong-yang, TAO Jin-zhang. Selective extraction of zinc, gallium, and germanium from zinc refinery residue using two stage acid and alkaline leaching [J]. Hydrometallurgy, 2019, 183: 38−44.
[24] HURŞIT M, LAÇIN O, SARAÇ H. Dissolution kinetics of smithsonite ore as an alternative zinc source with an organic leach reagent [J]. Journal of the Taiwan Institute of Chemical Engineers, 2009, 40(1): 6−12.
[25] LIU Fu-peng, LIU Zhi-hong, LI Yu-hu, WILSON B P, LUNDSTRÖM M. Extraction of Ga and Ge from zinc refinery residues in $H_2C_2O_4$ solutions containing H_2O_2 [J]. International Journal of Mineral Processing, 2017, 163: 14−23.
[26] DING Yun-ji, ZHANG Shen-gen, LIU Bo, LI Bin. Integrated process for recycling copper anode slime from electronic waste smelting [J]. Journal of Cleaner Production, 2017, 165: 48−56.

从锌置换渣中分段浸出锌、铅、镓和锗

饶 帅[1,2,3]，刘志强[1,2,3]，王东兴[1,2,3]，曹洪杨[1,2,3]，朱 薇[1,2,3]，张魁芳[1,2,3]，陶进长[1,2,3]

1. 广东省科学院 稀有金属研究所，广州 510650；
2. 广东省科学院 稀有金属分离与综合利用国家重点实验室，广州 510650；
3. 广东省科学院 广东省稀土开发及应用研究重点实验室，广州 510650

摘 要：采用分段浸出方法从锌置换渣中选择性提取锌、铅、镓和锗。首段浸出过程通过控制合适的硫酸浓度与液固比条件，锌和镓的浸出率达到90%和99%以上，超过92%的锗留在硫酸浸出渣中；二段采用盐酸作为浸出剂选择性提取铅，铅的浸出率为99%，锗损失率小于2%；三段采用1 mol/L氢氧化钠作为浸出剂，通过破坏硅锗固溶体的结构，实现锗高效溶出(90%)。对浸出渣进行物相分析，结果表明：三段浸出过程分别选择性溶解锌置换渣中硫酸锌、硫酸铅以及二氧化硅，实现锌、铅、镓和锗的高效溶出。上述分段浸出工艺为锌置换渣中有价金属高效回收提供了一条新思路。

关键词：锌置换渣；镓；锗；分段浸出

(Edited by Xiang-qun LI)